Published in final edited form as:
Nat Protoc. 2016 September ; 11(9): 1711–1723. doi:10.1038/nprot.2016.112.

A simple method for imaging axonal transport in ageing neurons using the adult *Drosophila* wing

Alessio Vagnoni and **Simon L. Bullock**
Division of Cell Biology, MRC Laboratory of Molecular Biology, Francis Crick Avenue, Cambridge, CB2 0QH, UK

Abstract

There is growing interest in the link between axonal cargo transport and age-associated neuronal dysfunction. Studying axonal transport in neurons of adult animals requires intravital or *ex vivo* imaging approaches, which are laborious and expensive in vertebrate models. We describe simple, non-invasive procedures for imaging cargo motility within axons using sensory neurons of the translucent *Drosophila* wing. A key aspect is a method for mounting the intact fly that allows detailed imaging of transport in wing neurons. Coupled with existing genetic tools in *Drosophila*, this is a tractable system for studying axonal transport over the lifespan of an animal and thus for characterising the relationship between cargo dynamics, neuronal ageing and disease. Preparation of a sample for imaging takes approximately 5 minutes, with transport typically filmed for 2–3 minutes per wing. We also document procedures for quantifying transport parameters from the acquired images and describe how the protocol can be adapted to study other cell biological processes in ageing neurons.

Introduction

Many cellular processes depend on the trafficking of organelles, vesicles and macromolecules by cytoskeletal motors. Neurons are particularly dependent on long-range cytoskeletal transport because of their remarkably elongated processes. It is therefore not surprising that defective axonal transport has been implicated in the pathogenesis of several age-related neurodegenerative diseases1. However, studying the relationship between axonal transport and the structure and function of the nervous system during ageing is challenging. This is chiefly due to difficulties in visualising transport within an adult animal.

Experimental systems have been described for imaging axonal transport in the nervous system of adult mice, which use either surgical procedures in whole animals2–5 or tissue explants6. Each of these methods is technically demanding and several involve invasive procedures. The long lifespan of mammals is a further challenge when studying the

Correspondence: avagnoni@mrc-lmb.cam.ac.uk or sbullock@mrc-lmb.cam.ac.uk.

Competing Financial Interests Statement
The authors declare that they have no competing financial interests.

Contributions
A.V. and S.L.B. conceived the study. A.V. and S.L.B. designed the experiments. A.V. performed the experiments and collected the data. A.V. and S.L.B. wrote the manuscript.

Europe PMC Funders Author Manuscripts

relationship between axonal transport and neuronal ageing. Here we describe a simple, non-invasive method for detailed characterisation of axonal transport in the intact nervous system of the fruit fly, *Drosophila melanogaster*. This system utilises the translucent adult wing to generate high quality image series of axonal cargo transport at different stages of adulthood. Importantly, the method can be combined with sophisticated genetic tools to study neurons that either lack or have reduced levels of specific proteins, or carry the equivalent of human disease mutations. This is therefore a tractable system for genetic and cell biological studies of how axonal cargo dynamics contribute to age-related neuronal dysfunction.

Development of the protocol and comparison to other methods

Third instar larval motor neurons of *Drosophila* have been used extensively for axonal transport studies because of the ability to combine fly genetics with detailed imaging of cargo dynamics (e.g. Refs. 7–9). However, this developmental system is not well suited for studying the relationship between axonal transport and neuronal ageing. We therefore sought to develop a protocol that allows detailed imaging of axonal transport in adult *Drosophila*. Our choice of the adult *Drosophila* wing was inspired by the publication of procedures for live imaging of sensory neurons within this system10–12. These methods were designed to visualise injury-induced axonal degeneration and have provided important insights into this process.

In the wing, the neurons are located within the costal vein and the longitudinal veins 1 (L1) and 3 (L3)13–15 (Fig. 1a). In the L1 vein, the neuronal cell bodies are located at the anterior wing margin, and are connected by short dendrites to mechanosensory and chemosensory bristles (Fig. 1b). The L3 vein contains fewer neurons, the sensilia of which are located in the proximal segment of the vein. The axons within each of the wing veins bundle together and project into the thoracic ganglion of the animal13–15.

One method for live imaging of wing neurons involves mounting whole flies in a block of agarose11,16. Although this procedure is suitable for axonal injury studies, we find that it is not compatible with detailed analysis of cargo transport within axons. Such analysis requires high magnification, high numerical aperture (NA) objectives. Because these objectives have a short working distance, they cannot be routinely used to visualise cargoes within the wings of flies mounted in an agarose block. Moreover, the agarose-based embedding procedure is time consuming (25–30 min per preparation), laborious, and subjects the tissue to large changes in temperature (incubating with 55°C agarose and cooling to 4°C or on ice). These temperature changes are likely to have consequences for cytoskeletal transport processes (e.g. microtubules depolymerise whilst kept at cold temperatures17,18). Wings that have been removed from the body of the fly have also been used for injury studies11,12. Unlike the agarose-block based method, this procedure makes it straightforward to mount wings flat, which facilitates imaging of the wing neurons. However, we have found that the dissection process leads to a rapid decline in mitochondrial transport in the axons of the wing neurons. Thus, this method is also not suitable for live imaging of axonal transport.

Our experiences with these preexisting methods led us to develop a new protocol that allows detailed visualisation of axonal cargoes within the wing sensory neurons of an intact fly (Fig. 1c, d). Whole flies are immobilised in a custom imaging chamber, which can be

quickly and easily constructed from coverslips and adhesive tape. Within each chamber, the most of each wing lays flat against a coverslip in halocarbon oil. Spinning disk-based imaging of these preparations produces high quality image series of axonal cargo transport. Overall, the mounting and imaging process takes less than 15 minutes per fly. We have also optimised procedures for extracting transport parameters from the image series.

Overview of the protocol

Our protocol consists of several different steps (Fig. 2). The first step is the generation of adult flies that express in wing neurons markers of specific cargoes that undergo microtubule-based transport. A range of fluorescent protein markers for axonal cargoes has been produced, with a large majority available through the Bloomington *Drosophila* Stock Center (Indiana University, IN; see also Table 1). Expression of the fluorescent protein is typically achieved with the binary *Gal4/UAS* expression system19 because of the large number of transgenic lines available. However, the orthogonal *lexA/lexAop* expression system20 can also be used effectively in wing neurons (see 'Experimental design' and 'Anticipated results' sections).

At each time point in the experiment, individual flies are mounted in the custom imaging chamber. Image series are promptly captured from these preparations and exported into open source software for manual tracking of cargo trajectories and subsequent extraction of transport parameters. The procedure can be repeated with flies at different stages of adulthood in order to evaluate transport dynamics during the ageing process.

Applications of the method

The major use of this method is the analysis of axonal transport in an adult model organism. Cohorts of flies can be collected from the same culture and aged for different lengths of time before imaging. This allows cargo dynamics to be characterised at a fixed time point or throughout the ageing process. We recently published a study that made extensive use of this protocol21. The study included the observation that the motility of mitochondria in wing neurons of young flies was comparable to the motility of these organelles in *Drosophila* larval motor neurons and the sciatic nerve of young mice. We also discovered that there is a boost and gradual decline in the frequency of mitochondrial movement within the axons of wing neurons during adult life. These changes did not reflect general changes in cargo transport, as the motility of dense-core vesicles was not altered over this period.

Importantly, the method can be combined with the sophisticated genetic tools previously established by the *Drosophila* community. It is possible to analyse how specific mutations affect transport processes by combining them with transgenes that mark cargoes fluorescently21. New mutations, including null mutations and single amino acid substitutions, can be generated rapidly using CRISPR/Cas9 genome engineering22,23. This affords the user many possibilities for functional studies, such as assessing how mutations that are associated with human neurological diseases affect axonal transport.

When mutations are not compatible with development of the fly to adult stages, or when it is important to discriminate cell autonomous and non-autonomous effects, tissue-specific analysis of gene function is possible through expression of RNAi constructs with *Gal4/*

*UAS*21. These RNAi constructs are available to the community from genome-scale collections24,25 and it is straightforward for a user to generate additional RNAi constructs for the same gene in order to control for potential off-target effects. If necessary, the timing of RNAi expression can be restricted using a temperature sensitive version of the Gal4 repressor, Gal80 ($Gal80^{ts}$)21,26,27. In these cases, it may be desirable to express fluorescent cargo markers using the *lexA/lexAop* system so that labelling is not under the same temporal control as the RNAi construct. Genetic stocks are also available to make fluorescently marked wing neurons that are homozygous for genetic mutations12. This provides an additional method to analyse the function of genes that have important roles in other *Drosophila* tissues.

In principle, the throughput of the assay also lends itself to pharmacological methods for manipulating protein function. Small molecule agonists or antagonists can be fed to flies by incorporation into yeast paste or fly food medium, followed by assaying the effects on cargo transport in wing neurons.

Finally, the ease of sample preparation and quality of imaging data afforded by the protocol means that it can be adapted to study other aspects of neuronal cell biology with high spatial and temporal resolution, including how these processes are influenced by changes in axonal transport. For example, we previously described fluorescent markers that can be used to assess age-associated focal protein accumulations in ageing neurons21. These can be used to correlate changes in transport processes with alterations in neuronal protein homeostasis. Expression of genetically encoded calcium sensors28,29, in combination with mechanical or chemical stimulation of wing margin bristles21,30, is a promising method for assessing neuronal activity during ageing and how it is altered by perturbations that influence transport. It should also be possible to use established fluorescent sensors of other cellular processes, such as oxidative stress31,32, in wing neurons.

Limitations

Manual tracking of single vesicles and organelles is time-consuming. Unfortunately, this is a common drawback for studies of cargo transport in different cell types. Although highly desirable, a reliable ‘universal’ method for automated particle tracking is currently not available. This is because tracking methods must be tailored to deal with sample specific differences such as signal-to-noise ratio, and cargo shape and density33–35. Currently, open-source software for automated tracking is unable to accurately measure transport parameters when applied to the wing neurons. Future efforts will be aimed at developing software that can perform this task.

A more specific drawback of the wing neurons is that, because of cuticular structures, immunostaining of whole-mount samples is not possible, at least with currently available protocols. However, a growing number of fluorescent markers is being generated by the *Drosophila* community, which will increase the versatility of our method. As described in Table 1, we have recently generated additional marker strains in our laboratory. Efficient genome editing in *Drosophila* by CRISPR/Cas9 and novel libraries of fluorescently tagged proteins (e.g. Ref. 36) will accelerate the production of fluorescent protein markers expressed at physiological levels.

Experimental design

Choice of fly strains **(Step 1)—**Table 1 documents a number of *Gal4/UAS* and *lexA/lexAop* strains that we have found are suitable for use with our protocol. The different *Gal4* and *lexA* driver strains differ in the proportion of neurons within the wing in which they are active11,12,14,21. Using a widely expressed driver together with an abundant cargo, such as mitochondria, can result in large datasets that increase statistical power. However, the density of cargoes in these genotypes means that accurate tracking of trajectories can be challenging and time-consuming. In this protocol we highlight some examples of transgene combinations with which we work routinely. However, the user should determine which transgenes are preferable for their specific needs.

Culturing flies **(Steps 2–5)—**Wherever possible, care should be taken to avoid changes in diet or environmental conditions during fly culture, as these could influence experimental outcomes. Thus, the food composition and preparation procedure should be kept constant during an entire study, with cohorts of control and experimental genotypes raised in parallel using the same batches of food. The temperature (25 ± 1ºC) and humidity (50 ± 3%) of our fly room is tightly controlled to minimise environmental changes.

Mounting of a fly in the imaging chamber **(Steps 8–19)—**The use of halocarbon oil is critical. The viscosity of the oil stabilises the body and the wings of the animal. This oil also allows diffusion of gases and, with a refractive index similar to glycerol, is an excellent choice for imaging studies37. We have used No. 0, No. 1 or No. 1.5 coverslips to construct the imaging chamber, and all give high quality images. We have noticed, however, that sealing the imaging chamber with an upper No. 1.5 coverslip occasionally results in damage to the fly. This is presumably due to excessive pressure exerted by this rigid coverslip. We therefore use No. 0 or No. 1 glass as the upper coverslip. The type of coverslips used to construct the chamber should be kept constant throughout each study to ensure consistent imaging. Although it is possible to mount several flies in each chamber, we advise against this practice as some flies will recover fully from the anaesthetic before imaging is complete; strong movements of the animal can affect the stability of the wing preparation and thus compromise imaging.

We typically expose a single fly to CO_2 for 4–5 minutes before mounting in the chamber in order to ensure long-term anaesthesia, followed by prompt imaging of wing neurons. In order to evaluate if long-term exposure to CO_2 affects transport in wing neurons, we performed control experiments in which flies were anaesthetised for only 20–30 seconds (the minimum time required to immobilise the fly and check wings for damage) before mounting and then allowed to recover from the anaesthetic for ~ 5 minutes prior to imaging. As expected, several preparations could not be used due to excessive movement of the fly. However, those preparations suitable for imaging had similar transport characteristics to those observed with longer CO_2 exposure (Supplementary Fig. 1). Thus, prolonged CO_2 treatment does not appear to affect transport processes in wing neurons.

Imaging **(steps 7 and 20–28)—**The use of high-magnification (60x or 100x), high numerical aperture objective lenses with apochromatic and flat field correction is crucial for

obtaining high quality image series of cargo transport. We typically use a 60x objective because, compared to the 100x, it has a relatively large depth-of-focus and field-of-view. A spinning disk imaging system is a critical part of the protocol, as this allows rapid, high signal-to-noise imaging of cargo transport in the wing with negligible photobleaching. Use of a laser scanning confocal microscope (e.g. LSM 780, Zeiss) at the same acquisition rates results in much noisier images that are not suitable for tracking cargo dynamics, and also causes substantial photobleaching. Several types of high quality spinning disk-imaging systems are commercially available, and it is likely that all of these can be used with this protocol for detailed analysis of cargo dynamics. Although most spinning-disk systems have an inverted configuration, it is also possible to use an upright configuration by flipping the orientation of the imaging chamber on the microscope stage.

The user should devote time to choosing optimal image acquisition settings for each fluorescent marker. These settings may need to be adjusted when expressing the same fluorescent protein with different drivers, as these will activate the target promoter to different degrees. Low frame rates can result in high signal-to-noise images that facilitate accurate assignment of cargo location in individual frames. However, if frame rates are too low, fine details of motion (e.g. short pauses and brief changes in direction) can be missed. Phototoxicity and photobleaching should also be taken into account when determining the acquisition parameters. Motility and morphology of mitochondria were not affected when the period of continuous imaging was extended to up to 30 min with our standard spinning disk acquisition parameters. We also did not observe a substantial amount of photobleaching of mitochondrial signals over this period, although bleaching may be more of an issue with cargoes that are bound by a small copy number of a fluorescent marker protein. We recommend choosing settings that allow the highest acquisition rate that is compatible with accurate tracking of motile cargoes throughout an image series.

The choice of the region of the wing to image has a large effect on the type of data produced. Imaging of neurons in the costal vein is challenging. Because the axons of these neurons bundle in close proximity to the thorax, they often do not lay flat against the coverslip. We therefore exclusively image the L1 or L3 veins. We favour imaging the arch region of L1 (Fig. 1a, c) because all the axons of this vein are collected in this segment. Thus, a large number of cargoes can be analysed from each movie. It is possible to image regions with fewer axons, for instance the region of the L1 vein in the distal part of the wing margin or the L3 vein (Fig. 1a, d). Having fewer cargoes per movie can simplify the tracking process, which can be beneficial when abundant cargoes are marked using a driver that is active in a large proportion of wing neurons. Once an area of the wing has been selected, it should be used throughout a study to control for any regional variation in transport dynamics.

The user should be aware that darkly pigmented regions of the wing, including the edge of the wing margin, are autofluorescent. However, this is not a substantial obstacle because these regions generally do not overlap with signals from axonal cargoes.

Ageing studies **(Step 6, 29)—**To analyse cargo transport at different stages post-eclosion, a cohort of flies is used that is collected from the same culture on the same day.

Typically, 6–10 flies are imaged for each condition (e.g. mutant and control genotypes) on each day of the experimental series. Although flies survive the mounting and imaging procedure and can be returned to culture vials, the residual oil means that wings often become folded or stuck to the body of the fly. It is therefore not practical to use the same flies for imaging on subsequent days. Because the variance in cargo transport dynamics between individual flies is small, other flies from the same cohort can reliably be used at the later time-points. In cases where it is desirable to image the same fly at a later time point – for example to evaluate cellular responses to a specific injury – the agarose-block mounting method11,16 may be preferable. This protocol allows extraction of the fly from the chamber and imaging for a second time, albeit with a risk of some flies dying or incurring damage to the wing11,16.

Quantification **(Steps 30–39)—**Kymographs cannot be used to accurately assign transport trajectories for abundant cargoes such as mitochondria due to the complexity of the traces produced. For consistency, we therefore use manual tracking of all cargoes in a study that includes analysis of abundant cargoes. Toggling back-and-forth between consecutive frames in the image series usually allows confident assignment of individual cargoes with this method. The ImageJ plugins MTrackJ38 and Manual Tracking (Fabrice Cordelières, Institute Curie, France) are well suited for manual tracking of image series. The two plugins offer different options in terms of data output, track recording and display. We favour MTrackJ for the more extensive array of parameters recorded.

A transported cargo is operationally defined as one containing at least one continuous movement of ≥ 2 μm, which we term a ‘run’. The start of a run is marked when a motile cargo enters the axonal segment or moves from a stationary position or into the focal plane for the first time. The run is terminated when the particle reaches the end of the axonal segment, stops or moves out of the focal plane. Anterograde and retrograde runs are those directed towards the thorax of the fly and the cell body of the neuron, respectively. We previously demonstrated that the microtubules in the axons of the wing neurons have a classical orientation, with plus ends extending away from the cell body21.

Materials

Reagents

- Transgenic flies for expressing the desired fluorescent marker protein in wing neurons (Table 1)
- ‘Iberian’ fly food (see Reagent Setup) Note that our protocol will also be compatible with other fly food recipes.
- Yeast (*Saccharomyces cerevisiae,* Type II, Sigma-Aldrich, cat. no. YSC2)
- Glucose (Formedium, cat. no. GLU03)
- Agar (*Drosophila* Agar Type II, Dutscher Scientific, cat. no. 789150)
- Organic plain white flour (BigBarn CIC, UK),
- Tegosept (Dutscher Scientific, cat. no. 789130) see Reagent Setup

- Propionic acid (Sigma-Aldrich, cat. no. P1386)
- Penicillin-Streptomycin (ThermoFisher Scientific, cat. no. 15140-122).
- Voltalef 10S halocarbon oil (VWR, cat. no. 24627.188)
- Absolute ethanol (Sigma, cat. no. 32221)

Equipment

Spinning-disk microscopy for time-lapse live imaging

- Inverted fluorescence microscope (Olympus IX71)
- Spinning disk imaging system (UltraVIEW ERS, PerkinElmer)
- Charge-coupled device (CCD) camera with 1344 x 1024 pixel chip (Orca ER, Hamamatsu)
- Mercury-Arc light source (Osram)
- 488 nm, 561 nm, 631 nm laser system (Melles Griot)
- 60x/1.4 NA and 100x/1.4 NA PlanApo oil-immersion objectives (Olympus)
- Stage-mounted slide clips (Olympus)
- Piezo objective positioner/scanner (Physik Instrumente) for *z*-stacks
- Immersion oil (e.g. Immersol 518F oil (Zeiss))

Confocal microscopy for acquisition of *z*-stacks (optional)—For end-point phenotypic analyses when time resolution is not crucial (e.g. quantifying protein aggregates), a laser scanning confocal microscope can also be used to acquire *z*-stacks.

- Confocal microscope (e.g. LSM 780, Zeiss)
- 63x/1.4 NA PlanApo oil-immersion objective (Zeiss)
- Immersion oil (e.g. Immersol 518F oil (Zeiss))

Software for image acquisition and quantification of transport

- ImageSuite software (PerkinElmer) for spinning disk system and ZEN software (Zeiss) for laser scanning confocal microscopy system
- ImageJ (Wayne Rasband, NIH, USA) (open source)
- ImageJ plugins: Straighten (Eva Kocsis, NIH, USA), StackReg (Philippe Thévenaz, EPFL, Switzerland), Image Stabilizer (Kang Li, Carnegie Mellon University, USA), Cell Counter (Kurt de Vos, University of Sheffield, UK), MTrackJ38, Manual Tracking (Fabrice Cordelières, Institute Curie, France) (all open source). Manuals for the use of the plugins are available at http://rsbweb.nih.gov/ij/plugins/.
- Excel (Microsoft)

- Prism (GraphPad)

Other equipment

- Disposable vials (Regina Industries, cat. no. P1066) and bungs (Genesee Scientific, cat. no. 59-201) for fly culture
- Electric table-top kettle (Cleveland Range, cat. no. KET-12-T) for preparation of fly food
- Dumont no. 5 fine forceps (Fine Science Tools, cat. no. 11251-20)
- Paper labelling tape (VWR, cat. no. 817-0027) and double-sided Sellotape (Banner Business Services, cat. no. 0603015) for constructing imaging chamber
- Coverslips No. 0 (22 x 64 mm, Scientific Laboratory Supplies, cat. no. MIC3208), No. 1 (22 x 64 mm, Scientific Laboratory Supplies, cat. no. MIC3228) or No. 1.5 (22 x 64 mm, Scientific Laboratory Supplies, cat. no. MIC3248) for assembly of the imaging chamber
- Paint brushes (ProArte, Prolene Plus Series 007, Size 3/0, cat. no. 50655182)
- Carbon dioxide supply for anaesthetising flies
- Dissecting stereomicroscope (e.g. Leica MZ7.5) for mounting anaesthetised flies in the imaging chamber
- (Optional) 215 automatic Liquid Handler (Gilson, cat.no. 2510121) for aliquoting fly food.

Reagent Setup

Tegosept stock solution—Dissolve 50 g of Tegosept powder in 500 ml of absolute ethanol (Sigma, cat. no. 32221) to give a 100 mg/ml stock solution.

‘Iberian’ fly food—70 mg/ml yeast, 55 mg/ml glucose, 7.7 mg/ml agar, 35 mg/ml organic plain white flour, 1.2 mg/ml Tegosept, 0.4% (vol/vol) propionic acid, 100 U/ml Penicillin-Streptomycin. For a 5 L batch: Heat 3 L tap water to ~ 110°C using an electric table-top kettle; Add 275 g glucose and 350 g yeast, stir the mixture and boil for 15 min; Stir 38.5 g agar into 800 ml room temperature (~ 22–23°C) tap water and add to the hot glucose/yeast/water mixture; Stir the mixture and boil for 20 min; Add 175 g flour to 800 ml room temperature tap water, stir and add to the previous agar/glucose/yeast/water mixture; Stir the mixture and boil for 30 min; Add room temperature tap water to a final volume of 5 L; Cool mixture to between 55°C and 60°C; Add 60 ml Tegosept stock solution, 20 ml propionic acid and 50 ml Pen/Strep solution (10,000 U/ml), followed by mixing; Decant into culture vials manually or using a 215 automatic Liquid Handler. Allow solution to set and top each vial with a bung. Store fly food at 4°C for up to two weeks and warm to room temperature before use.

Europe PMC Funders Author Manuscripts

Equipment Setup

Imaging chamber—The imaging chamber can be partially assembled as described in Steps 13 and 14 of the 'Procedure'. Partially assembled chambers can be kept indefinitely in a coverslip box until required.

Procedure

Fly husbandry. TIMING typically 10–66 days after setting up the parental crosses

1| Cross male and virgin female flies to produce progeny expressing fluorescent markers in wing neurons (see Table 1).

CRITICAL STEP Crosses should be designed so that the flies that will be imaged do not contain genetic markers that strongly affect wing morphology (e.g. *CyO* balancers). Such markers necessitate unnatural flattening of the wing during mounting, which can damage the tissue and thus compromise the transport process.

CRITICAL STEP In order to reach meaningful conclusions, there must be sufficient agematched flies for statistical comparisons between the control and experimental conditions. When only a proportion of the offspring will have the desired genotype, the scale of fly crosses should be increased accordingly.

2| Maintain the crosses at 25°C with a 12-h-light/12-h-dark cycle. If temperature sensitive experiments are performed (e.g. control of transgene expression via the Gal4 repressor $Gal80^{ts}$) rear the flies at the appropriate temperature.

3| Closely monitor the fly cultures so as not to miss the day when the first adult flies eclose.

4| Transfer newly emerged flies of the desired genotype to a vial with fresh food at the end of the day using standard *Drosophila* handling procedures. Record which day each cohort of flies eclosed.

CRITICAL STEP Do not collect too many flies in a single culture vial as overcrowding can increase the rate of lethality (we usually keep < 20 flies per vial, with males and females cultured in the same vial).

5| If necessary, collect newly emerged flies on subsequent days at the same time to establish additional cohorts. Alternatively, collect flies every 8–12 h for fine-grained analysis of transport properties.

CRITICAL STEP During the first 24–48 hours after eclosion from the pupal case, transport dynamics of at least some cargoes in the wing nerve change dramatically21. We therefore recommend collecting cohorts of flies every 8–12 h during this period. It is also possible to mount flies of newly eclosed flies as soon as the wings unfold21.

6| For ageing studies, carefully transfer the flies into vials with new food once or twice per week following anaesthetisation with CO_2.

CRITICAL STEP Regular transfer of flies to new vials minimises the risk of wings being damaged by contact with fly food that has been churned up by larvae.

Preparation for imaging, assembly of the imaging chamber and fly mounting TIMING typically less than 10 min.

7| Turn on the laser, mercury light source, microscope and acquisition software. Rotate the objective turret so that the desired objective is positioned below the stage opening. Set the acquisition parameters in the software.

CRITICAL STEP Ensure the temperature of the room is kept constant as cellular processes, including the activity of microtubule motors, may be sensitive to any changes in this parameter. The temperature of our microscope room is maintained at 21–22°C by the building's environmental control system.

8| Anaesthetise the flies from the desired culture on a CO_2 pad. See Supplementary Video 1 for a demonstration of steps 8–19.

9| Using a stereomicroscope, inspect flies for any abnormalities in their wings (e.g. cuts, blisters or folds).

10| Choose a single fly without wing abnormalities for imaging and return the other flies to the food vial.

CRITICAL STEP The sex of the fly imaged for each movie should be recorded so that potential sex-specific outcomes can be evaluated later (note that the dynamics of mitochondrial transport are indistinguishable in male and female flies21).

11| Keep the selected fly on the CO_2 pad for 4–5 min.

CRITICAL STEP If necessary to ensure long-term anaesthetisation, flies can be treated with CO_2 for longer. The user should check that the animal survives extended treatment with CO_2 and should keep the anaesthetisation conditions constant within the same experimental series.

12| Gather the equipment needed to assemble the imaging chamber (Fig. 3a–f). The first part of the chamber assembly (Steps 13 and 14, Fig. 3a–c) can be completed during the anaesthetisation process. For convenience, part built chambers (Fig. 3a and b) can be prepared in advance.

13| Make a stack of three layers of paper labelling tape on each of the short sides of a coverslip (Fig. 3a). Each piece of labelling tape has dimensions of ~ 15 mm x 7 mm. The labelling tape stacks act as spacers for the imaging chamber.

CRITICAL STEP The number of layers required in the stacks can vary depending on the thickness of the batch of labelling tape. An appropriate stack thickness ensures that the fly is lightly restrained once the chamber is sealed with an upper coverslip, such that the legs are prevented from moving without the body of the animal being damaged by excessive squeezing.

14| Add a single layer of double-sided tape to each of the two stacks of labelling tape, as well as to the centre of the coverslip. This latter piece is aligned with its long axis perpendicular to the long axis of the coverslip (Fig. 3b). When part-built chambers are made in advance, the paper layer protecting the outer adhesive part of double-sided tape should not be removed until the chamber is needed.

15| Use a paintbrush to apply a thin coat of 10S halocarbon oil to a small region of the coverslip adjacent to the central piece of double-sided tape (Fig. 3c).

16| Following the anaesthetisation period, pick up the fly by gently holding the legs with the forceps. Lower the fly towards the coverslip with the dorsal side leading.

17| Apply the fly to the region of coverslip with the halocarbon oil so that the dorsal side of the head is gently pressed against the central piece of double-sided tape and the dorsal side of the rest of the fly is positioned against the glass (Fig. 3d). The double-sided tape helps stabilise the fly during imaging. Make sure the wings are extended away from the thorax, lying completely flat against the coverslip. If this does not occur naturally, the position of the wings can be adjusted very carefully with a paintbrush (see Supplementary Video 1 for an example).

CRITICAL STEP Apply just enough oil for the wings to remain attached to the coverslip. Excessive oil will prevent the entire wing from abutting the coverslip, which leads to problems with focusing and sample drift during imaging.

CRITICAL STEP We advise against using glues, such as Dermabond 2-octyl cyanoacrylate39, to stabilise the wings. Glues can affect the integrity of the thin wing tissue, resulting in detrimental effects on axonal transport.

? TROUBLESHOOTING

18| Gently apply a thin layer of halocarbon oil on top of the wings with a fine paintbrush.

CRITICAL STEP Be careful not to damage or stretch the wings during this process. Too thick a layer of oil can lead to wings lifting up from the coverslip.

? TROUBLESHOOTING

19| Seal the chamber by attaching a second coverslip on top of the two tape stacks at either end of the first coverslip (Fig. 3e). To do so, apply by hand one end of the upper coverslip to one stack and gently lower the other end of the upper coverslip on top of the second stack. Once loosely applied, press the upper coverslip gently above the positions of the tape stacks.

CRITICAL STEP The pressure exerted on the upper coverslip should be just enough to restrain the movement of the fly’s legs. Applying excessive pressure

may damage the fly. Uneven pressure on the upper coverslip may cause the fly to tilt sidewise, in which case it may not be possible to image transport.

Imaging TIMING usually less than 10 min per fly

20| Carefully pick up the imaging chamber by hand and promptly transfer it to the room containing the spinning disk imaging system attached to an inverted microscope (in our case, this is adjacent to the sample preparation room). Add a small amount of immersion oil to the 60x or 100x objective and position the imaging chamber above the stage opening with the lower coverslip (i.e. the one supporting the wing) facing the objective. We secure the imaging chamber with stage-mounted slide clips, but adjustable slide holders can also be used.

21| Use the X-Y translational controls on the stage to position the fly above the objective**,** using the bright-field configuration to locate one of the wings in the eyepieces. Inspect the wing for signs of damage that may have been missed at the stereomicroscope. Image the other wing if damage to the first wing is found. If both wings are damaged, discard the chamber and return to step 8.

CAUTION Because excessive pressure of the objective can lead to fracture of the chamber, the fine focus adjustment should be used when the objective is close to the surface of the imaging chamber.

22| Find the desired area of the wing using landmarks shown in Fig. 1a (see ‘Experimental Design’ for the advantages and disadvantages of imaging from different regions).

CRITICAL STEP Film the same region of the wing for an entire experimental series in order to control for region-specific differences in transport parameters.

23| Position the microscope filters to allow fluorescence imaging with the wavelength appropriate for the cargo marker. Adjust the focus based on the fluorescent signal.

? TROUBLESHOOTING.

24| Turn on the ‘Acquisition’ mode of the imaging software. Re-adjust laser intensity, exposure time, camera gain and the size of the imaging window if necessary. Keep imaging settings constant for an experimental series.

? TROUBLESHOOTING.

25| Initiate time-lapse image acquisition with continuous illumination and a total capture time as desired. We routinely image mitochondrial transport (e.g. using *dpr-Gal4, UAS-mito::GFP* or *Appl-Gal4, UAS-mito::GFP*) for 3 min with a capture rate of 0.5 frame/s and the transport of faster cargoes, such as dense core-vesicles (e.g. using *Appl-Gal4, UAS-ANF::EMD*), for 2 min with a capture rate of 1 frame/s.

? TROUBLESHOOTING

26| Repeat steps 21–25 for the other wing of the mounted fly, provided visual inspection reveals no damage. In our experience, there are no overt differences in transport dynamics between the first and second wing that is imaged.

27| Discard the chamber at the end of imaging in accordance with local safety protocols.

28| Repeat steps 8–27 for several flies on the same day.

29| For ageing studies, repeat steps 7–28 on additional days using flies from the same cohort.

Quantification of transport TIMING variable, depending on the dataset; 20–40 min per movie is typical for a dataset with a large number of cargoes (e.g. 50–60/frame)

30| Export image series from the imaging system's computer to the analysis station.

31| Open an image series in ImageJ.

32| If the image series has been exported as multiple frames, use the 'Images to Stack' function to create a stack (Image -> Stacks -> Images to Stack).

33| If necessary, use the Straighten plugin to straighten any axonal curvature (Plugins -> Straighten).

34| If the sample has drifted in the X-Y plane during imaging, stabilise the straightened image with the StackReg or Image Stabilizer plugin (Plugins -> StackReg or Plugins -> Image Stabilizer).

35| Crop all images in the image series to the same area for consistency. We routinely quantify transport from an axon segment of 50-μm in length. If desired, kymographs can be plotted using the Kymograph Creator function of ImageJ.

36| Track transported cargoes with MTrackJ (Plugins -> MTrackJ). Manually determine the start and end of each run and use the plugin to determine the cargo's centroid position at each point. Use the Cluster tool in MTrackJ to group different categories of motion (e.g. anterograde, retrograde and bidirectional cargoes) so they can be evaluated separately in steps 38 and 39. Adjust the brightness and contrast of the movie while manually tracking as this helps follow dim particles.

CRITICAL STEP Track all motile particles that are visible in the image series to avoid any sub-conscious bias that could occur if a subset of particles is randomly selected for analysis.

? TROUBLESHOOTING

37| Use the Cell Counter plugin (Plugins -> Cell Counter) to mark the total number of particles from a representative frame. This value is used to calculate the percentage of the population that is motile.

CRITICAL STEP When adjacent organelles are very close or touching, toggle back-and-forth between neighbouring frames in the image series to identify whether single or multiple particles are present at a specific point.

38| Export the recorded dataset into Excel and calculate the desired mean values (± errors) per cargo per wing. We routinely evaluate the mean and distribution of velocities and run lengths (anterograde and retrograde), as well as the mean number and percentage of motile cargoes.

39| Export the datasets created in Excel into Prism in order to generate graphs and perform statistical analyses. Use a post-hoc correction method for multiple comparisons when performing statistical evaluations with several groups.

? TROUBLESHOOTING

Troubleshooting

Troubleshooting advice can be found in Table 2.

Timing

Steps 1–6 and 29: Timing depends on the time of eclosion and the age of the flies analysed; typically 10–66 days after beginning parental cross (based on eclosion from the pupal case 10 days after egg laying at 25ºC and longitudinal studies of up to 8 weeks)

Steps 7–19: Typically 5–10 min.

Steps 20–28: Typically less than 10 min per fly

Steps 30–39: Timing depends on the dataset; 20–40 min per movie for a dataset with a large number of cargoes

Anticipated Results

By following the mounting and imaging procedures in this protocol, we can routinely visualise axonal transport dynamics with high spatial and temporal resolution. The quality of the image series allows accurate manual tracking of cargo trajectories, which can be used to evaluate changes that occur at different stages of the animal's lifetime and in specific genetic backgrounds. The mounting procedure that we present in this protocol is also suitable for super-resolution microscopy, as demonstrated by the structured illumination microscopy (SIM) image in Supplementary Fig. 2.

Fig. 1c, d and Supplementary Videos 2 and 3 show representative examples of wing neurons with GFP- or mCherry-labelled mitochondria, which were captured with spinning disk microscopy. The quality of images also allows other dynamic events to be captured, such as mitochondrial fission and fusion (Fig. 4; Supplementary Videos 4 and 5). Fig. 1c and d and Supplementary Videos 2 and 3 illustrate the difference in the number of cargoes in a field of view when imaging the arch region of the L1 vein and the L3 vein. As described in

Europe PMC Funders Author Manuscripts

‘Experimental Design’, imaging the L3 vein is an option when the high density of cargoes in the arch region makes tracking of an entire image series challenging or time-consuming.

As also described in ‘Experimental Design’, an alternative strategy for manipulating the density of cargoes in a field of view is the use of drivers that are expressed in only a subset of sensory neurons within the L1 vein. For example, the expression patterns of *dpr-Gal4* and *ok371-Gal4* are more restricted than those of the pan-neuronal drivers such as *elav-Gal4*, *Appl-Gal4 and nSyb-lexA*. Fig. 5a provides an example of different densities of fluorescent cargoes when imaging the same region of the wing with a restricted (*dpr-Gal4*) and more widespread (*Appl-Gal4*) driver line.

The importance of choosing an appropriate driver line for specific experimental situations is further exemplified in Fig. 5b and Supplementary Video 6. The presence of a closely linked *UAS-GFP* transgene on the *dpr-Gal4* chromosome makes it very challenging to track small cargoes that are labelled with a green fluorescent fusion protein (e.g. GFP, YFP or Emerald). This is because the background fluorescence from the *UAS-GFP* masks the fluorescence of the cargo marker (Fig. 5b). This is not an issue when imaging mitochondria with *dpr-Gal4*, presumably as these organelles contain many copies of the fluorescent marker protein. The use of an alternative driver is therefore recommended for tracking small cargoes labelled with green fluorescent proteins (Fig. 5c and Supplementary Video 7). Alternatively, small cargoes can be marked by red fluorescent proteins (e.g. RFP or mCherry) under the control of *dpr-Gal4* (Fig. 5d and Supplementary Video 8).

In summary, the protocol presented here is a simple and versatile method for analysing axonal transport in the context of an ageing animal. Coupling the imaging procedures to established genetic tools in *Drosophila* has the potential to provide important insights into the relationship between axonal transport and the function of adult neurons, including in the context of ageing and disease.

Supplementary Material

Refer to Web version on PubMed Central for supplementary material.

Acknowledgements

We are grateful to the LMB Media Kitchen for fly food preparation, Neil Grant from LMB Visual Aids for help with Figure 3 and Supplementary Video 1, Mathias Pasche (MRC-LMB) for assistance with the SIM experiments, and Damian Brunner, Greg Jefferis, Alex Whitworth and the Bloomington *Drosophila* Stock Center (Indiana University, IN) for sharing fly stocks. The development of this protocol was supported by funding to S.L.N. from the UK Medical Research Council [MRC file reference number MC_U105178790]. A.V. is the recipient of an NC3Rs David Sainsbury Fellowship [NC/N001753/1].

References

1. Millecamps S, Julien J-P. Axonal transport deficits and neurodegenerative diseases. Nat Rev Neurosci. 2013; 14:161–176. [PubMed: 23361386]
2. Misgeld T, Kerschensteiner M, Bareyre FM, Burgess RW, Lichtman JW. Imaging axonal transport of mitochondria *in vivo*. Nat Methods. 2007; 4:559–561. [PubMed: 17558414]
3. Sajic M, et al. Impulse conduction increases mitochondrial transport in adult mammalian peripheral nerves *in vivo*. PLoS Biol. 2013; 11:e1001754. [PubMed: 24391474]

Europe PMC Funders Author Manuscripts

4. Gibbs KL, Kalmar B, Sleigh JN, Greensmith L, Schiavo G. *In vivo* imaging of axonal transport in murine motor and sensory neurons. J Neurosci Methods. 2016; 257:26–33. [PubMed: 26424507]
5. Takihara Y, et al. *In vivo* imaging of axonal transport of mitochondria in the diseased and aged mammalian CNS. Proc Natl Acad Sci USA. 2015; 112:10515–10520. [PubMed: 26240337]
6. Milde S, Adalbert R, Elaman MH, Coleman MP. Axonal transport declines with age in two distinct phases separated by a period of relative stability. Neurobiol Aging. 2015; 36:971–981. [PubMed: 25443288]
7. Rao S, Lang C, Levitan ES, Deitcher DL. Visualization of neuropeptide expression, transport, and exocytosis in *Drosophila melanogaster*. J Neurobiol. 2001; 49:159–172. [PubMed: 11745655]
8. Gunawardena S, et al. Disruption of Axonal Transport by Loss of Huntingtin or Expression of Pathogenic PolyQ Proteins in *Drosophila*. Neuron. 2003; 40:25–40. [PubMed: 14527431]
9. Pilling AD, Horiuchi D, Lively CM, Saxton WM. Kinesin-1 and Dynein are the primary motors for fast transport of mitochondria in *Drosophila* motor axons. Mol Biol Cell. 2006; 17:2057–2068. [PubMed: 16467387]
10. Fang Y, Soares L, Teng X, Geary M, Bonini NM. A novel *Drosophila* model of nerve injury reveals an essential role of Nmnat in maintaining axonal integrity. Curr Biol. 2012; 22:590–595. [PubMed: 22425156]
11. Fang Y, Soares L, Bonini NM. Design and implementation of in vivo imaging of neural injury responses in the adult *Drosophila* wing. Nat Protoc. 2013; 8:810–819. [PubMed: 23589940]
12. Neukomm LJ, Burdett TC, Gonzalez MA, Züchner S, Freeman MR. Rapid in vivo forward genetic approach for identifying axon death genes in *Drosophila*. Proc Natl Acad Sci USA. 2014; 111:9965–9970. [PubMed: 24958874]
13. Whitlock KE, Palka J. Development of wing sensory axons in the central nervous system of *Drosophila* during metamorphosis. J Neurobiol. 1995; 26:189–204. [PubMed: 7535838]
14. Nakamura M, Baldwin D, Hannaford S, Palka J, Montell C. Defective proboscis extension response (DPR), a member of the Ig superfamily required for the gustatory response to salt. J Neurosci. 2002; 22:3463–3472. [PubMed: 11978823]
15. Fang Y, Bonini NM. Hope on the (fruit) fly: the *Drosophila* wing paradigm of axon injury. Neural Regen Res. 2015; 10:173–175. [PubMed: 25883604]
16. Soares L, Parisi M, Bonini NM. Axon Injury and Regeneration in the Adult *Drosophila*. Sci Rep. 2014; 4:6199. [PubMed: 25160612]
17. Cassimeris LU, Wadsworth P, Salmon ED. Dynamics of microtubule depolymerization in monocytes. J Cell Biol. 1986; 102:2023–2032. [PubMed: 3519619]
18. Fygenson D, Braun E, Libchaber A. Phase diagram of microtubules. Phys Rev E Stat Phys Plasmas Fluids Relat Interdiscip Topics. 1994; 50:1579–1588. [PubMed: 9962129]
19. Brand AH, Perrimon N. Targeted gene expression as a means of altering cell fates and generating dominant phenotypes. Development. 1993; 118:401–415. [PubMed: 8223268]
20. Lai S-L, Lee T. Genetic mosaic with dual binary transcriptional systems in *Drosophila*. Nat Neurosci. 2006; 9:703–709. [PubMed: 16582903]
21. Vagnoni A, Hoffmann PC, Bullock SL. Reducing Lissencephaly-1 levels augments mitochondrial transport and has a protective effect in adult *Drosophila* neurons. J Cell Sci. 2016; 129:178–190. [PubMed: 26598558]
22. Port F, Chen H-M, Lee T, Bullock SL. Optimized CRISPR/Cas tools for efficient germline and somatic genome engineering in *Drosophila*. Proc Natl Acad Sci USA. 2014; 111:E2967–E2076. [PubMed: 25002478]
23. Xu J, et al. A Toolkit of CRISPR-Based Genome Editing Systems in *Drosophila*. J Genet Genomics. 2015; 42:141–149. [PubMed: 25953352]
24. Dietzl G, et al. A genome-wide transgenic RNAi library for conditional gene inactivation in *Drosophila*. Nature. 2007; 448:151–156. [PubMed: 17625558]
25. Ni JQ, et al. A *Drosophila* resource of transgenic RNAi lines for neurogenetics. Genetics. 2009; 182:1089–1100. [PubMed: 19487563]
26. Suster ML, Seugnet L, Bate M, Sokolowski MB. Refining GAL4-driven transgene expression in *Drosophila* with a GAL80 enhancer-trap. Genesis. 2004; 39:240–245. [PubMed: 15286996]

27. Pfeiffer BD, et al. Refinement of tools for targeted gene expression in *Drosophila*. Genetics. 2010; 186:735–755. [PubMed: 20697123]
28. Chen T-W, et al. Ultrasensitive fluorescent proteins for imaging neuronal activity. Nature. 2013; 499:295–300. [PubMed: 23868258]
29. Dana H, et al. Sensitive red protein calcium indicators for imaging neural activity. eLife. 2016; 5:e12727. [PubMed: 27011354]
30. Valmalette JC, et al. Nano-architecture of gustatory chemosensory bristles and trachea in *Drosophila* wings. Sci Rep. 2015; 5:14198. [PubMed: 26381332]
31. Albrecht SC, Barata AG, Grosshans J, Teleman AA, Dick TP. *In vivo* mapping of hydrogen peroxide and oxidized glutathione reveals chemical and regional specificity of redox homeostasis. Cell Metab. 2011; 14:819–829. [PubMed: 22100409]
32. Chatterjee N, Bohmann D. A versatile ΦC31 based reporter system for measuring AP-1 and Nrf2 signaling in *Drosophila* and in tissue culture. PloS One. 2012; 7:e34063. [PubMed: 22509270]
33. Reis GF, et al. Molecular motor function in axonal transport in vivo probed by genetic and computational analysis in *Drosophila*. Mol Biol Cell. 2012; 23:1700–1714. [PubMed: 22398725]
34. Chenouard N, et al. Objective comparison of particle tracking methods. Nature methods. 2014; 11:281–289. [PubMed: 24441936]
35. Bros E, Hauser A, Paul F, Niesner R, Infante-Duarte C. Assessing Mitochondrial Movement Within Neurons: Manual Versus Automated Tracking Methods. Traffic. 2015; 16:906–917. [PubMed: 25903548]
36. Nagarkar-Jaiswal S, et al. A genetic toolkit for tagging intronic MiMIC containing genes. eLife. 2015; 4:e08469.
37. Parton RM, Vallés AM, Dobbie IM, Davis I. Isolation of *Drosophila* egg chambers for imaging. Cold Spring Harb Protoc. 2010; 2010doi: 10.1101/pdb.prot5402
38. Meijering E, Dzyubachyk O, Smal I. Methods for cell and particle tracking. Methods Enzymol. 2012; 504:183–200. [PubMed: 22264535]
39. Chatzigeorgiou M, Bang S, Hwang SW, Schafer WR. tmc-1 encodes a sodium-sensitive channel required for salt chemosensation in *C. elegans* . Nature. 2013; 494:95–99. [PubMed: 23364694]
40. Torroja L, Chu H, Kotovsky I, White K. Neuronal overexpression of APPL, the *Drosophila* homologue of the amyloid precursor protein (APP), disrupts axonal transport. Curr Biol. 1999; 9:489–493. [PubMed: 10322116]
41. Lin DM, Goodman CS. Ectopic and increased expression of fasciclin II alters motoneuron growth cone guidance. Neuron. 1994; 13:507–523. [PubMed: 7917288]
42. Mahr A, Aberle H. The expression pattern of the *Drosophila* vesicular glutamate transporter: a marker protein for motoneurons and glutamatergic centers in the brain. Gene Expr Patterns. 2006; 6:299–309. [PubMed: 16378756]
43. Pfeiffer BD, Truman JW, Rubin GM. Using translational enhancers to increase transgene expression in *Drosophila*. Proc Natl Acad Sci USA. 2012; 109:6626–6631. [PubMed: 22493255]
44. Fabrowski P, et al. Tubular endocytosis drives remodelling of the apical surface during epithelial morphogenesis in *Drosophila* . Nat Commun. 2013; 4:2244. [PubMed: 23921440]
45. Akerboom J, et al. Optimization of a GCaMP calcium indicator for neural activity imaging. J Neurosci. 2012; 32:13819–13840. [PubMed: 23035093]
46. Halfon MS, et al. New fluorescent protein reporters for use with the *Drosophila* Gal4 expression system and for vital detection of balancer chromosomes. Genesis. 2002; 34:135–138. [PubMed: 12324968]
47. Lee T, Luo L. Mosaic Analysis with a Repressible Cell Marker for Studies of Gene Function in Neuronal Morphogenesis. Neuron. 1999; 22:451–461. [PubMed: 10197526]
48. Petersen LK, Stowers RS. A Gateway MultiSite recombination cloning toolkit. PloS One. 2011; 6:e24531. [PubMed: 21931740]
49. Han C, Jan LY, Jan Y-N. Enhancer-driven membrane markers for analysis of nonautonomous mechanisms reveal neuron-glia interactions in *Drosophila* . Proc Natl Acad Sci USA. 2011; 108:9673–9678. [PubMed: 21606367]

50. Yang W-K, et al. Nak regulates localization of clathrin sites in higher-order dendrites to promote local dendrite growth. Neuron. 2011; 72:285–299. [PubMed: 22017988]
51. Barolo S, Castro B, Posakony JW. New *Drosophila* transgenic reporters: insulated P-element vectors expressing fast-maturing RFP. Biotechniques. 2004; 36:436–442. [PubMed: 15038159]
52. McGuire SE, Le PT, Osborn AJ, Matsumoto K, Davis RL. Spatiotemporal rescue of memory dysfunction in *Drosophila*. Science. 2003; 302:1765–1768. [PubMed: 14657498]

Europe PMC Funders Author Manuscripts

Europe PMC Funders Author Manuscripts

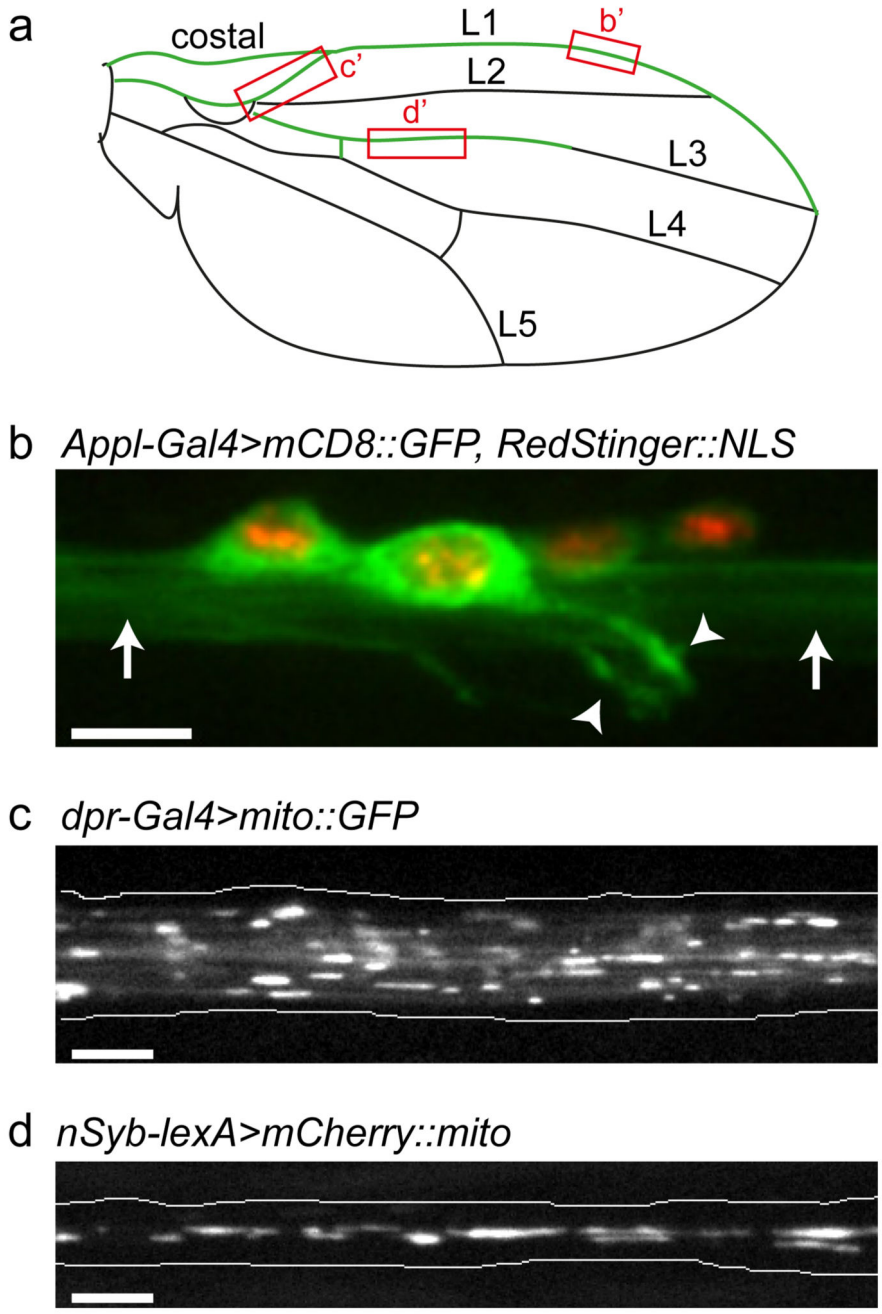

Figure 1. Imaging organelle transport in the nervous system of the adult *Drosophila* wing.

(**a**) Cartoon of the *Drosophila* wing showing the position of the costal and longitudinal veins (L1–L5). The nervous system is highlighted in green. Boxes highlight regions imaged in **b**–**d**. (**b**) Cell bodies and processes of L1 vein neurons. Green, cell membranes; red, nuclei (genotype is *Appl-Gal4>mCD8::GFP, RedStinger::NLS*). Arrowheads, dendrites; arrows, bundled axons. (**c**) Still image of GFP-labelled mitochondria in axons of the wing arch region of a *dpr-Gal4>mito::GFP* fly one day after eclosion (from Supplementary Video 2). (**d**) Still image of mCherry-labelled mitochondria in axons of the L3 vein of a *nSyb-*

lexA>mCherry::mito fly two days after eclosion (from Supplementary Video 3). Images in **b**–**d** were captured with spinning disk microscopy using the procedures described in the protocol (**b**, *z*-stack projection; **c** and **d**, single focal planes). Scale bars: 5 μm.

Europe PMC Funders Author Manuscripts

Europe PMC Funders Author Manuscripts

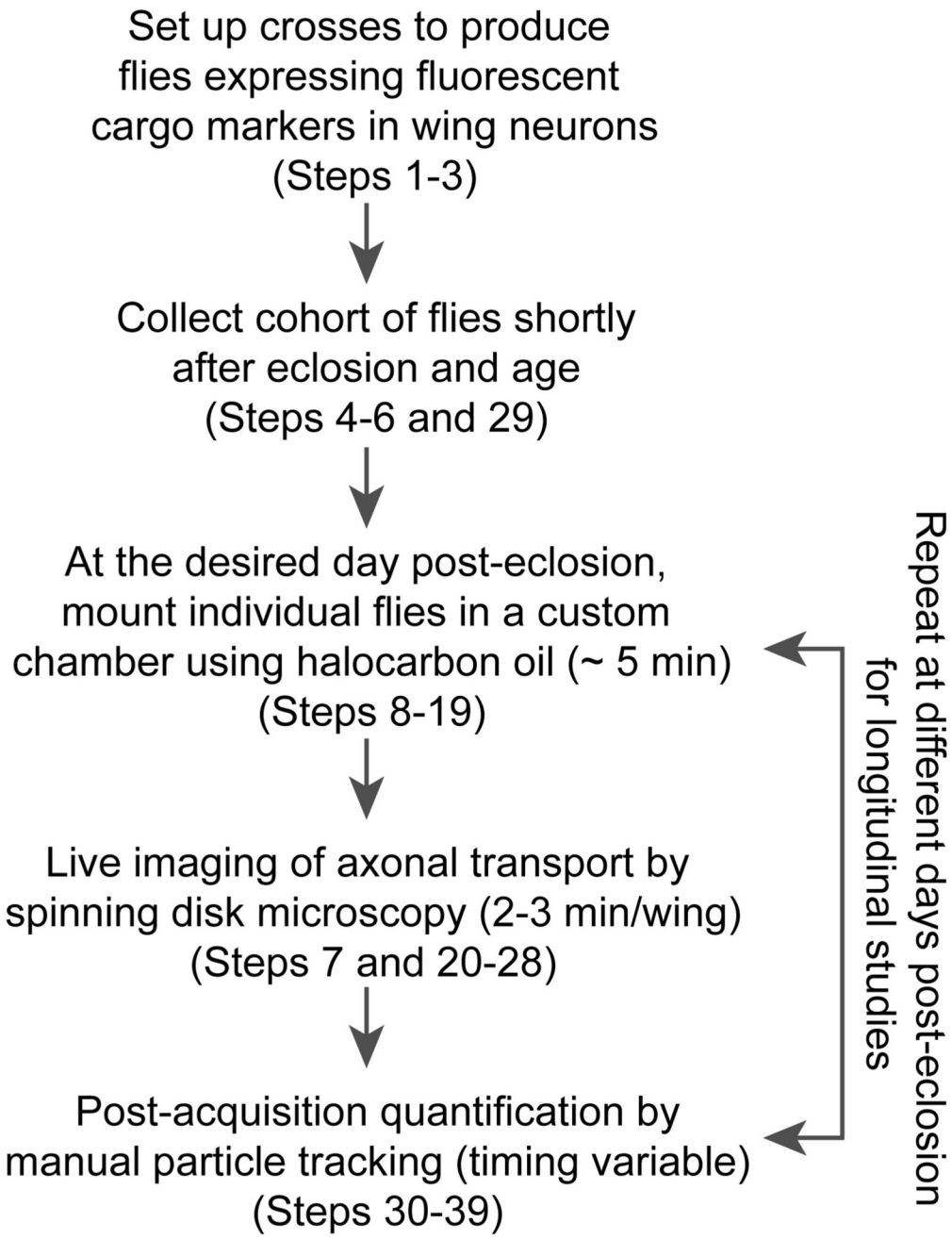

Figure 2. Overview of the experimental procedure.

As detailed in the ‘Procedure’ section, the total experimental time is variable depending on how long the flies are aged after eclosion and the number, length and complexity of the movies that need to be tracked.

Europe PMC Funders Author Manuscripts

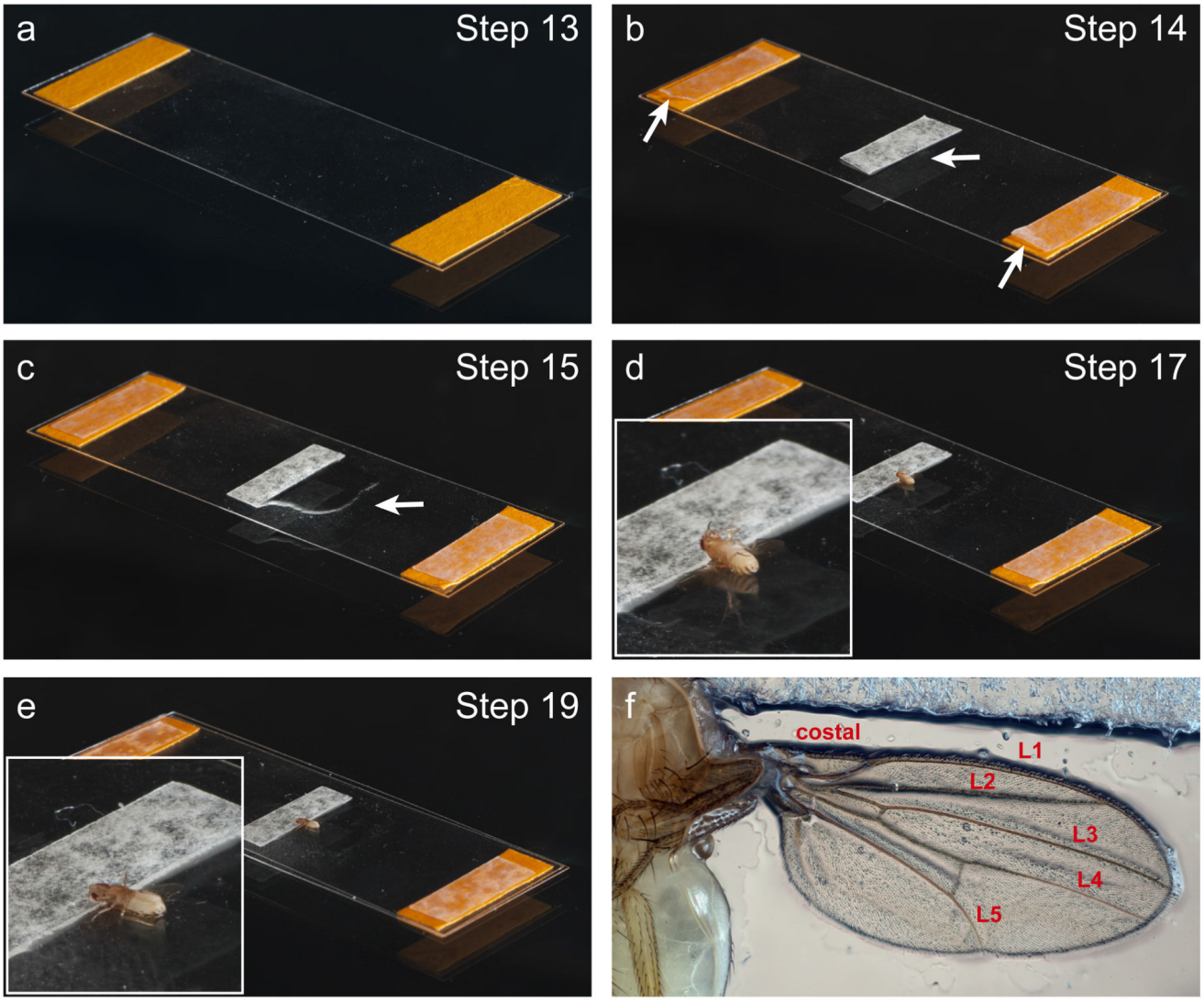

Figure 3. Key steps in the preparation of the imaging chamber

(**a**) Two stacks of labelling tape (orange) are attached to a coverslip. (**b**) A single layer of double-sided tape (marked by arrows) is added to each of the two stacks of labelling tape, as well as to the centre of the coverslip. (**c**) Halocarbon oil is applied to a small region of the coverslip (arrow). (**d** and inset) The fly is mounted dorsal side down on the coverslip, with the head stuck to the double-sided tape and the wings extended over the surface of the glass. (**e** and inset) A second coverslip seals the chamber, gently pressing against the fly. See Supplementary Video 1 for more details of these procedures. (**f**) Photograph of a wing mounted in the chamber. Wing veins are labelled as in Fig. 1a.

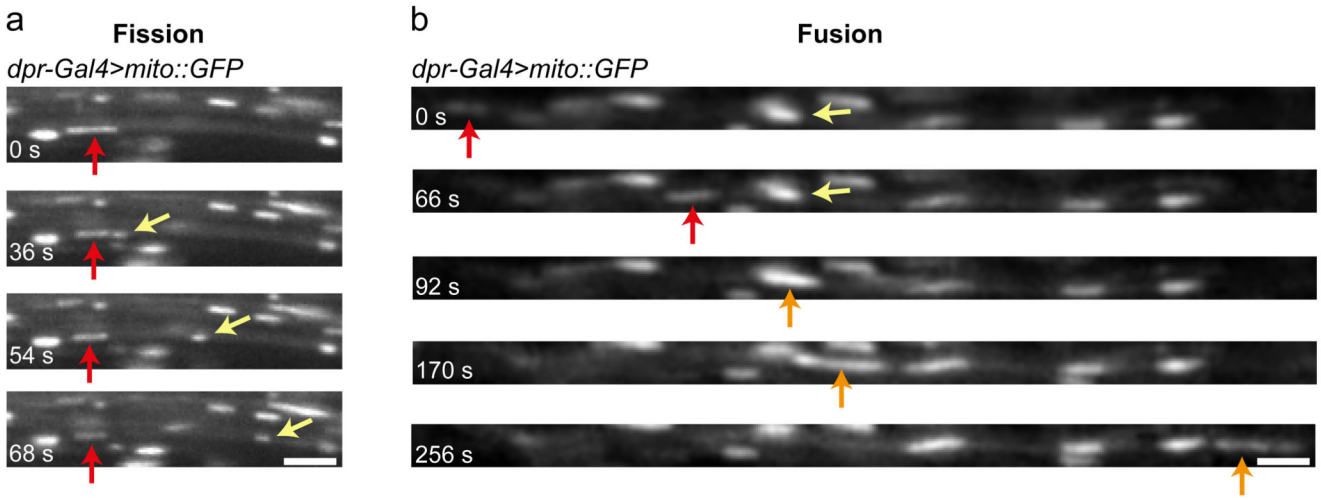

Figure 4. Visualisation of mitochondrial fission and fusion events in wing neurons.

Still images showing examples of mitochondrial fission (**a**) and fusion (**b**) in the L1 vein of *dpr-Gal4>mito::GFP* flies (taken from Supplementary Videos 4 and 5, respectively). (**a**) A stationary GFP-marked mitochondrion (red arrow) undergoing fission. The newly generated, motile mitochondrion is marked by a yellow arrow. (**b**) Example of mitochondrial fusion between a motile (red arrow) and a stationary (yellow arrow) mitochondrion. The orange arrow marks the newly generated mitochondrion, which is motile. Scale bars: 2.5 μm.

Europe PMC Funders Author Manuscripts

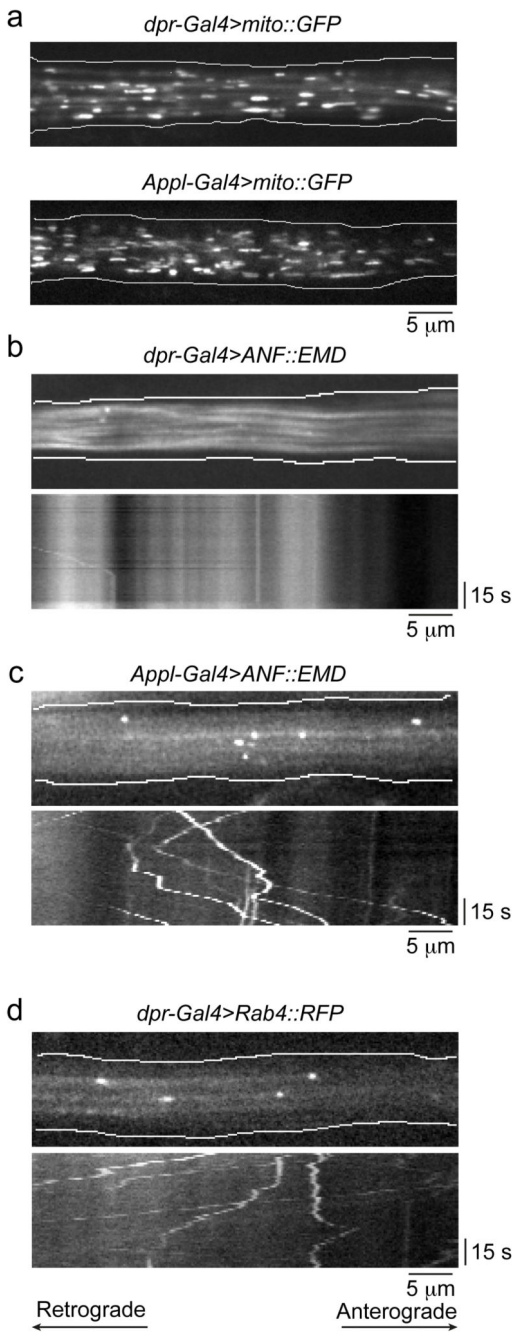

Figure 5. Representative results with different combinations of drivers and cargo markers in wing neurons.

(**a**) Still images of GFP-marked mitochondria using *dpr-Gal4* (top panel) and *Appl-Gal4* (bottom panel), illustrating the increased number of mitochondria visualised with the latter, pan-neuronal driver. (**b**, **c**) Illustration of the importance of choosing an appropriate driver strain when imaging small cargoes labelled with green fluorescent proteins. Top images in **b** and **c** show a still image from Supplementary Videos 6 and 7, respectively, in which the dense-core vesicle marker prepro-atrial natriuretic factor peptide (ANF)::Emerald (EMD) is

expressed with *dpr-Gal4* (**b**) or *Appl-Gal4* (**c**). The bottom images in each panel show kymographs from Supplementary Video 6 and 7, respectively. The *dpr-Gal4* chromosome has a *UAS-GFP* transgene closely linked to the *Gal4* transgene, which gives cytoplasmic GFP background that prevents tracking of EMD-labelled dense-core vesicles. (**d**) *dpr-Gal4* can be used to label small cargoes with red fluorescent proteins. Top image, still image from Supplementary Video 8 showing $Rab4^{+}$ endosomes that are marked with RFP using this driver. Bottom image, kymograph from Supplementary Video 8. All images in the figure are from the arch region of the L1 vein. The retrograde and anterograde directions are towards the left and right of the images, respectively.

Europe PMC Funders Author Manuscripts

Table 1

Examples of transgenic fly lines that can be used to label cargoes fluorescently in wing neurons

Strain	Purpose	BDSC No.([a])	Reference
Drivers:			
Appl-Gal4	Pan-neuronal GAL4 expression (chemosensory and mechanosensory wing neurons)	32040	(40)
dpr-Gal4 ([b])	GAL4 expression in chemosensory neurons	25083	(14)
elav^{C155}-Gal4	Pan-neuronal GAL4 expression (chemosensory and mechanosensory wing neurons)	458	(41)
ok371-Gal4	GAL4 expression in glutamatergic neurons	26160	(42)
nSyb-lexA	Pan-neuronal LexA expression (chemosensory and mechanosensory wing neurons)	52817	(43)
Fluorescent reporters ([c]):			
UAS-ANF::EMD	Marks dense-core vesicles	7001	(7)
UAS-App::YFP	Marks APP-positive vesicles	32039	(8)
UAS-Eb1::GFP	Marks growing plus ends of microtubules	-	(44)
UAS-GalT::RFP	Marks Golgi vesicles	30908	Donated to BDSC by J. Lippincott-Schwartz
UAS-GCaMP5G	Intracellular Ca^{2+} reporter	42037	(45)
UAS-GCaMP6F	Intracellular Ca^{2+} reporter	42747	(28)
UAS-GFP	Marks entire cytoplasm	6658	(46)
UAS-mCD8::GFP	General marker of membranes	5130	(47)
UAS-mCD8::ChRFP ([d])	General marker of membranes	27392	(48; donated to BDSC by F. Schnorrer)
UAS-mCD4::tdTomato	General marker of membranes	35837; 35841	(49)
UAS-mito::GFP	Marks mitochondria	8442; 8443	(9)
UAS-mCherry::mito ([e])	Marks mitochondria	-	This study
UAS-Rab4::RFP	Marks Rab4-positive endosomes	8505	(50)
UAS-RedStinger::NLS	Marks nuclei	8546	(51)
lexAop-GFP	Marks entire cytoplasm	-	(43)
lexAop-mCherry::mito ([e])	Marks mitochondria	-	This study
Other			
tub-Gal80^{ts}	Temperature sensitive version of GAL4 repressor	7016	(52)

[a] BDSC, Bloomington *Drosophila* Stock Center. See BDSC website for full genotypes;

[b] contains a closely linked *UAS-GFP* transgene (see Fig. 5b);

[c] *UAS* and *lexAop* lines are used with GAL4 and LexA, respectively;

[d] also forms some cytoplasmic aggregates even in young flies;

[e] unlike mito::GFP, in which GFP is targeted to the mitochondrial matrix using a sequence from human cytochrome C oxidase subunit VIII, mCherry::mito is anchored on the mitochondrial outer membrane using the *Drosophila* Miro transmembrane domain.

Table 2

Troubleshooting table.

Step	Problem	Possible reason	Solution
17–18	Fly is not stably attached to the coverslip	Too much oil applied	Start again with a new fly, reducing amount of oil on the coverslip and/or on the wings
23	Difficulty focusing on an axonal segment of sufficient length	Wing not mounted flat	i) Make sure wings are properly extended during mounting. ii) Reduce amount of oil on the coverslip and/or on the wings during mounting
		Wing is drifting excessively	Reduce amount of oil on the coverslip and/or on the wings during mounting
		Fly is moving	Keep flies on the CO_2 pad for longer than 5 min before mounting
24	Images are dim	Laser power, camera gain or exposure time is too low	Increase laser power, camera gain and exposure time accordingly
		Fluorescent signal from cargo not bright enough	(i) Try other drivers as these may give higher expression levels. (ii) Try an alternative fluorescent protein (or concatemers of fluorescent proteins)
25	Few motile cargoes visible in the field of view	Choice of wing region with relatively few axons	Choose a different area. The number of axons in the proximal L1 vein (wing arch) is greater than in the distal L1 vein or L3 vein
		Choice of driver that is active in a subset of wing neurons	Use a driver that is active in a broader population of neurons (Table 1)
		Cytoplasmic background when using the *dpr-Gal4 UAS-GFP* chromosome to image small, green fluorescent cargoes	Use a different driver or a red fluorescent marker protein
		Fly is not of an optimal age	Image flies at 1–2 d after eclosion, when transport of all organelles imaged to date is robust
36	Too many particles moving makes accurate tracking difficult and time-consuming	Choice of wing region with a relatively high number of axons	Choose a different area. The number of axons in the distal L1 vein or L3 vein is less than in the proximal L1 vein (wing arch)
		Choice of driver that is active in a broad set of wing neurons	Use a driver that is active in a subset of neurons (Table 1)
39	Large variability in transport parameters between flies of the same genotype	Mounting of flies not performed consistently	Practise mounting procedure. Take care not to damage the wings during mounting
		Flies imaged are of a different age	Pay attention to the timing of eclosion; if required, establish a cohort of flies that eclosed in a narrow time window
		Imaging settings are not constant	Keep the same acquisition settings (e.g. laser power, acquisition time and camera gain) throughout
		Changes in temperature	Keep flies at a constant temperature throughout the experiment